

All-day uninterrupted power generator: Harvesting energy from the sun and cold space

Shuai Zhang

Shanghai Jiao Tong University

Zhenhua Wu

Shanghai Jiao Tong University

Zekun Liu

Shanghai Jiao Tong University

Erzhen Mu

Henan Polytechnic University

Yang Liu

Shanghai Jiao Tong University

Yongbo Lv

Shanghai Jiao Tong University

Thomas Thundat

University at Buffalo, The State University of New York

Zhiyu Hu (✉ zhiyuhu@sjtu.edu.cn)

Shanghai Jiao Tong University

Research Article

Keywords: photothermal conversion, radiative cooling, thermoelectric generator

Posted Date: August 23rd, 2021

DOI: <https://doi.org/10.21203/rs.3.rs-832470/v1>

License:  This work is licensed under a Creative Commons Attribution 4.0 International License.

[Read Full License](#)

Abstract

Harvesting energy from the environment to generate electricity is attracting tremendous interest to enrich the forms of energy utilization, reduce greenhouse gas emissions and alleviate the global energy crisis^{1,2}. However, achieving an unlimited and uninterrupted all-day power generation from the ambient energy is still challenging³. Herein, we demonstrate a passive power device to harvest energy from the sun and cold space based on micro-fabricated thermoelectric generator (TEG) integrated with solar absorber (SA) and radiative cooling emitter (RCE) to realize continuous power generation from the ambient. The ultrathin TEG, that with a sensitivity of 10^{-4} K achieved output power density of 960 W/m^3 while heated to 80°C at room temperature. The solar absorber (SA) performs photothermal conversion to heat the TEG in the daytime⁴, while the radiative cooling emitter (RCE) radiates the heat to the cold space through the atmospheric window to cool the TEG all the clear day^{5,6}. Our strategy provides a renewable and sustainable thermodynamic resource to build a temperature difference over TEG for all-day uninterrupted power generation for wide application scenarios. This is the first proof-of-principle uninterrupted power generation system independent of time on a small scale, and opportunities exist for environmental energy harvesting and electricity generation beyond traditional technologies.

Introduction

Carbon neutrality provides an effective strategy to solve the global warming and environmental problems accompanying economic growth and social development, which requires the society to reduce the excessive dependence on traditional non-renewable energy and enhance the utilization of new sustainability energy. Over the past few decades, the development of renewable natural sources such as solar, hydroelectric, marine, geothermal and wind has contributed positively to reduce global carbon emissions^{1,2,7}, but these technologies are restricted by time and space, and can only alleviate local energy shortages⁸⁻¹¹. Achieving uninterrupted power supply without time and space constraints will help promote world-wide access to energy source but still remain a major challenge.

A thermoelectric generator (TEG) is an energy harvester that convert environmental thermal energy to electrical energy directly based on the Seebeck effect¹²⁻¹⁷, providing an alternative approach for how to solve the need for unlimited continuous energy supply. The integration of TE modules in practical devices is one of the primary factors limiting its performance. Another key strategy for remarkable electricity output is to build enough temperature difference across the TEG. The sun, as the most typical huge heat source ($\sim 5800\text{K}$) outside the earth, has been used as the hot side of the TEG combined with solar absorber (SA) which convert the solar energy into heat by photothermal effect^{4,18-21}. A temperature increase of $40 \sim 60^\circ\text{C}$ under 1-sun irradiation can be achieved by utilizing these materials as efficient photothermal converters due to their plasmon resonance effect and by intrinsic absorption and increased thermal motion^{18,22,23}. However, TEG integrated with SA has a good power generation effect only in the daytime, and fails during nighttime.

Recently, a passive radiative cooling strategy has been adopted to cool buildings without any electricity input, which uses the coldness of the universe (3 ~ 4 K) to radiate the heat from terrestrial objects in the form of infrared radiation through the atmospheric window (7 ~ 14 μm)^{5,6,24-26}. Interestingly, this cooling strategy can be utilized to create temperature drops and thus provide a cold source for the TEG to generate electricity^{27,28}. However, this kind of generator has the unique advantage at the nighttime than daytime, because the heating under direct sunlight will weaken the cooling effect^{29,30}. Therefore, designing an all-day power generator remains a key challenge for a sustainable energy future.

Here, we report on a device capable of all-day self-generation power which harvests the energy from the sun and cold space. Anodic aluminum oxide coated with polyaniline nanoparticles (PANI@AAO) was used as a solar absorber (SA) to convert the solar energy into heat, which generates a temperature increase of 60°C under one sun illumination. A planar polydimethylsiloxane (PDMS) -Ag based radiative cooling emitter (RCE) was used to realize continuous cooling with an optimal temperature drop of 6°C on a typical clear day. Finally, we fabricated an ultrathin highly integrated TEG which was sandwiched between the SA and RCE with the RCE facing the sky. A spontaneous all-day temperature difference was produced across the TEG to drive the directional movement of the carriers within it, thereby realizing electricity generation outdoors throughout the day. This all-day uninterrupted power generator that harvest energy from the sun and cold space provide exciting opportunities for new renewable power generation, and shows huge potential for wide application scenarios such as industrial and residential communities as well as unmanned distributed power source for electronic components.

Results And Discussion

Based on a strategy of the synergy of materials and micro-nano structures to enhance the light-trapping effect and photothermal conversion performance^{31,32}, we polymerized the photothermal material-polyaniline (PANI) in-situ on a commercial nanoporous anodic aluminum oxide (AAO) with vertical channels (Figure S1-S3). The PANI nanoparticles completely cover the surface of the AAO template and are randomly distributed on the inner walls of the vertical holes as shown in Fig. 1a. When light falls onto the PANI@AAO, it will be reflected and gradually absorbed by the structure. This AAO vertical channels with large aspect ratio and abundant rough PANI nanoparticles attached form optical traps to capture light efficiently, and thus is an ideal solar absorber (SA) with a near-perfect black surface in a wide spectral range (from 300 ~ 2500 nm) (Fig. 1b). What is more, the PANI@AAO converts the solar energy into heat owing to the lattice vibrations and localized surface plasmon resonance (LSPR) effect. Under one sun illumination (1000 W/m²), the surface temperature of the PANI@AAO exhibits a significant increase and eventually reaches an equilibrium value of 82°C. As the intensity of sunlight increases, the surface of the sample can reach a higher equilibrium value which shows the potential to obtain a higher temperature by using concentrator optics (Fig. 1c).

The net heating power of the SA for the outdoor performance (under the standard AM1.5 sunlight) under different environmental parameters and various weather conditions was simulated based on a theoretical

thermal measurement model as shown in Fig. 1d (more details are given in Figure S4). The heat exchange process between the SA and environment has been taken into account in the theoretical simulation. A maximum net heating power of 830 W/m^2 can be achieved at room temperature (298 K). With the increase in temperature, the collective effect of nonradiative heating (conductive and convective heating) increases, leading to a decrease of the net heating power.

Passive radiative cooling emitters (RCE) can shed the heat of ground objects to the ultra-cold space by taking advantage of the thermal radiation through the atmospheric transparency window from $7 \sim 14 \mu\text{m}$, thereby cooling the objects and its surrounding environment^{33,34}. In this work, we fabricated a typical RCE (PDMS backed with a 100-nm-thick silver thin film, the silver reflect solar irradiation as a metallic mirror) on a silicon wafer (Fig. 2a-b). The optical properties of the device were investigated in the standard AM1.5 solar spectrum and the long wave infrared (LWIR) atmospheric transparency window. The complete emissivity/absorptivity spectrum across an ultrabroadband wavelength range in the solar and the mid-infrared regions of the RCE is shown in Fig. 2c. The RCE shows minimal absorption from 300 nm to $2.5 \mu\text{m}$, where the solar spectrum is located, and possesses a nearly saturated emissivity of 92% in the LWIR atmospheric transparency window ($7 \sim 14 \mu\text{m}$). The real-time temperature tracking of the air and the RCE that exposed to sky were measured to investigate the actual cooling capability during 24 h in Shanghai, China. The RCE can achieve a sub-ambient temperature drop of $\sim 6^\circ\text{C}$, especially at nighttime, showing a steady and sustained cooling effect as shown in Fig. 2d. However, considering the complexity of the daytime environment under direct sunlight, the measured cooling performance of the RCE was fluctuated.

Theoretically, the terrestrial radiative cooling effect comes from the imbalance of radiative heat flow between the sky-facing object and cold space, and the atmospheric transparency window providing a major channel for ground objects to radiate heat into the cold space with low losses. Figure 2e shows the net cooling power of the RCE during daytime and nighttime for various values of h_c (nonradiative heat coefficient) that ranged from 0 to $7 \text{ W/m}^2/\text{K}$ (more details are given in Figure S5). Obviously, the RCE could achieve a maximum cooling power in excess of 120 W/m^2 making a theoretically possibility for nighttime operation as $h_c \rightarrow 0$ (the solid line in Fig. 2e). The degree of solar absorption by the RCE has an inversely adverse implication on its achievable cooling powers. What is more, when the surface temperature of the RCE is above or close to ambient temperature, the emitter cooler has a stronger sub-ambient cooling effect.

TEG is a kind of energy harvester that can convert thermal energy into electrical energy directly based on Seebeck effect, and have been considered as one of the most promising and environmental-friendly power devices for the future. For current commercial TEG, its improvement is limited by the innovation and the development of highly integrated nano/micro-devices which allows for larger series structures can take advantage of small temperature differences. With the development of Micro-Electro-Mechanical System (MEMS) and thin film deposition technology, the design and preparation of large array nano/micro-devices with high integration degree have gradually become a reality. Based on our previous

work³⁵, an ultrathin MEMS-TEG on a 1×0.7 cm rectangular silicon wafer at the chip level was fabricated along with further increasing the thickness of TE materials. The MEMS-TEG is composed of 572 P-N ($\text{Sb}_2\text{Te}_3\text{-Bi}_2\text{Te}_3$) modules in series, and the size of each P/N leg is 200 μm ×200 μm ×1 μm (length×width×thickness) (Fig. 3a, the inset of Fig. 3b and Figure S6). The measured open-circuit voltage and output power of the TEG as a function of varied temperature from 40 to 160°C is shown in Fig. 3b and Figure S7. The open-circuit voltage increases with temperature and reaches a value as high as 8 mV at $T \approx 160^\circ\text{C}$. Meanwhile, a power output of about 0.4 μW could be achieved when the external load resistance matches the internal resistance of the device of about 70 Ω . The bulk power density of the MEMS-TEG (with a volume of $4.6 \text{ E}^{-11} \text{ m}^3$ including electrodes and thermoelectric materials) achieved 5.5 kW/m^3 when its hot end temperature is 140 °C with an active heat source and the cold end faces the air. Figure 3c shows the stability of the ultrathin TEG under relatively small temperature difference of 1.5°C, indicating the reliability of long-term operation. The wide operating temperature range and efficient power output capability represent the practical application potential of the MEMS-TEG.

Owing to the characteristics of ultra-thin and high integration, the MEMS-TEG is extremely sensitive to small temperature difference. Interestingly, when a hand or ice gets close to the MEMS-TEG, it will send back an obvious voltage signal (Fig. 3d). In a word, both thermal and cold stimuli will create a temperature difference across the MEMS-TEG, resulting in a voltage output (with a typical sensitivity of 10^{-4} K based on a total Seebeck coefficient of 200 $\mu\text{V}/\text{K}$ of one TE pair). Because the ultrathin MEMS-TEG could utilize such a tiny temperature difference, it has great potential in the special fields of self-powered nano-micro devices, environmental energy utilization, industrial waste heat utilization and distributed generation.

By careful integration of the SA and the RCE to the two ends of the TEG, an uninterrupted power generation SA-RCE-TEG that utilizes photo-thermal effect, radiation cooling and thermoelectric effect is realized. As shown in Fig. 4a, the SA converts the solar energy into heat energy in a clear daytime and thus provide a heat source for TEG. Meanwhile, the RCE function as a metallic mirror strongly reflecting the sunlight and selectively radiating the heat into the cold outer space in the form of infrared radiation throughout the day, and thus provided a continuous cold source for TEG. In the whole thermal dynamic process, the TEG acts as an energy converter that provide a channel for directional heat transmission to form a stable temperature difference between the upper and lower surfaces, thus realizing continuous electric power output.

In this hybrid system, during the daytime, SA absorbs sunlight as a heat source and is the main temperature difference generator. But at nighttime, because there is no sun, RCE is the only contributor of temperature difference. More importantly, due to the disappearance of solar radiation, the cooling effect of RCE in nighttime is better than that in the daytime. Figure 4a shows the basic scheme of all-day self-powered energy harvesting system in a building roof, and Fig. 4b is the real-time temperature and output voltage of continuous outdoor test for more than 4 days (more details show in Figure S8-S10). In particular, because the heating power of the SA is much greater than the cooling power of the RCE, the

SA-RCE-TEG has a higher surface temperature and temperature difference in the daytime. What is remarkable is that the SA-RCE-TEG can not only achieve up to a 120 μV output voltage ($\sim 1.1 \text{ W/m}^3$) during daytime, but also produce an 8 μV stable output voltage ($\sim 5.0 \text{ mW/m}^3$) at night, showing the viability of all-day continuous environmental thermal energy harvesting and outdoor electricity generation. However, compared to the single TEG with an active heat source ($T_{\text{hot}}=80^\circ\text{C}$, $T_{\text{cold}}=25^\circ\text{C}$, $P_{\text{out}}=960 \text{ W/m}^3$), the performance of SA-RCE-TEG with similar temperature of environmental energy source ($T_{\text{SA}}=82^\circ\text{C}$, $T_{\text{RCE}}=20^\circ\text{C}$, $P_{\text{out}}=1.1 \text{ W/m}^3$) is insufficient. This demonstrates that, with better thermal management and good thermoelectric materials may increase the output power of the next generation of devices. The sustainable output electricity of the SA-RCE-TEG could be collected to power nano-micro electronic devices, especially for the special scenes, such as harsh and remote environment.

Conclusion

In summary, we have demonstrated and fabricated a self-generation thermoelectric generator (SA-RCE-TEG) based on photothermal effect and radiation cooling effect for all-day uninterrupted efficient power generation. The SA consisting of AAO templates and PANI nanoparticles exhibits excellent light trapping performance, super absorbance and high photothermal conversion efficiency ($T_{\text{SA}}=82^\circ\text{C}$). A typical silicone PDMS film backed with silver film on a silicon wafer served as RCE, enabling a high solar reflectance and mid-infrared emittance ($T_{\text{drop}}=6^\circ\text{C}$). Further, we have demonstrated the heating and the sub-ambient cooling effect of these two devices theoretically and experimentally. Particularly, an ultrathin MEMS thermoelectric device with a sensitivity of 10^{-4} K was fabricated and achieved output power density of 960 W/m^3 while heated to 80°C at room temperature. The TEG was sandwiched between the SA (heater) and RCE (cooler), which provide a channel for heat flow directional transmission, thus forming temperature difference and generating electricity. Real-time all-day uninterrupted power generation of this SA-RCE-TEG device was experimentally demonstrated on consecutive days including typical sunny and cloudy days. In this work, we propose a transformative concept of simultaneous harvesting the hotness/coldness from the sun/space as a renewable and sustainable energy source to build temperature difference on ultrathin MEMS-TEG to realize power generation without any mechanical vibration and greenhouse gas emission. In a word, this proposed integrated generator provide deep insight into the continuous capture and utilization of environmental energy, and have disruptive potentials in mitigating the energy crisis and global warming.

Declarations

Acknowledgements

This work was supported by the National Natural Science Foundation of China (grant no.: 51776126). We would like to thank the Center of Advanced Electronic Materials and Devices and Instrumental Analysis Center of Shanghai Jiao Tong University for providing experimental test support. We also thank Prof. Kasper Moth-Poulsen and Prof. Yanzhong Pei for reading and commenting on this manuscript.

Author contributions

Supervisor: Z. Hu

Conceptualization: S. Zhang, Z. Wu and Z. Hu

SA fabrication: S. Zhang and Y. Lv

MEMS-TEG fabrication: Z. Liu, E. Mu and Y. Liu

RCE fabrication: S. Zhang

Characterization: S. Zhang and Z. Wu

Modeling and simulation: E. Mu and Y. Lv

Writing: S. Zhang and Z. Wu

Review and editing: T. Thundat and Z. Hu

Competing interest declaration

The authors declare no competing financial interest.

Additional information

The Supporting Information is available free online. Including materials, measurements, experimental details, theoretical model and references.

Corresponding author

Zhiyu Hu: zhiyuhu@sjtu.edu.cn

References

1. Dresselhaus, M. S. & Thomas, I. L., Alternative energy technologies. *Nature* **414**, 332–337 (2001).
2. Sinsel, S. R., Riemke, R. L. & Hoffmann, V. H. Challenges and solution technologies for the integration of variable renewable energy sources-A review. *Renew. Energ.* **145**, 2271–2285 (2020).
3. Chen, Z. et al. Simultaneously and synergistically harvest energy from the sun and outer space. *Joule* **3**, 101–110 (2019).
4. Kraemer, D. et al. High-performance flat-panel solar thermoelectric generators with high thermal concentration. *Nat. Mater.* **10**, 532–538 (2011).
5. Raman, A. P., Li, W. & Fan, S. H. Generating light from darkness. *Joule* **3**, 2679–2686 (2019).

6. Yin, X. B. et al. Terrestrial radiative cooling: Using the cold universe as a renewable and sustainable energy source. *Science* **370**, 786–791(2020).
7. Chu, S. & Majumdar, A. Opportunities and challenges for a sustainable energy future. *Nature* **488**, 294–303 (2012).
8. Chen, G. R. et al. Smart textiles for electricity generation. *Chem. Rev.* **120**, 3668–3720 (2020).
9. Zhang, C. G. et al. Bifilar-pendulum-assisted multilayer-structured triboelectric nanogenerators for wave energy harvesting. *Adv. Energy Mater.* **11**, 2003616 (2021).
10. Yu, B. Y. et al. Thermosensitive crystallization-boosted liquid thermocells for low-grade heat harvesting. *Science* **370**, 342–346 (2020).
11. Wang, Z. H. et al. Macroscopic heat release in a molecular solar thermal energy storage system. *Energy Environ. Sci.* **12**, 187–193 (2019).
12. Shi, X. L., Zou, J. & Chen, Z. G. Advanced thermoelectric design: From materials and structures to devices. *Chem. Rev.* **120**, 7399–7515 (2020).
13. Li, D. L. et al. Recent progress of twodimensional thermoelectric materials. *Nano-Micro Lett.* **12**, 36 (2020).
14. Zhou, W. N. et al. Seebeck-driven transverse thermoelectric generation. *Nat. Mater.* **20**, 463–467 (2021).
15. Han, C. G. et al. Giant thermopower of ionic gelatin near room temperature. *Science* **368**, 1091–1098 (2020).
16. Zhang, X. et al. Electronic quality factor for thermoelectrics. *Sci. Adv.* **6**, eabc0726 (2020).
17. Qiu, J. H. et al. 3D Printing of highly textured bulk thermoelectric materials: mechanically robust BiSbTe alloys with superior performance. *Energy Environ. Sci.* **12**, 3106–3117 (2019).
18. Ding, T. P. et al. Hybrid photothermal pyroelectric and thermogalvanic generator for multisituation low grade heat harvesting. *Adv. Energy Mater.* **8**, 1802397 (2018).
19. Zong, L. et al. Intensifying solar-thermal harvest of low-dimension biologic nanostructures for electric power and solar desalination. *Nano Energy* **50**, 308–315 (2018).
20. Jung, Y. S. et al. Wearable solar thermoelectric generator driven by unprecedentedly high temperature difference. *Nano Energy* **40**, 663–672 (2017).
21. Li, Z. Q. et al. A solar thermoelectric nanofluidic device for solar thermal energy harvesting. *CCS Chem.* **2**, 2174–2182 (2020).
22. Xu, D. X. et al. Insights into the photothermal conversion of 2D MXene nanomaterials: Synthesis, mechanism, and applications. *Adv. Funct. Mater.* **30**, 2000712 (2020).
23. Zhang, Q., Xu, W. L. & Wang, X. B. Carbon nanocomposites with high photothermal conversion efficiency. *Sci. China Mater.* 2018, 61, 905–914 (2018).
24. Hossain, M. M. & Gu, M. Radiative cooling: Principles, progress, and potentials. *Adv. Sci.* **3**, 1500360 (2016).

25. Zhao, B. et al. Radiative cooling: A review of fundamentals, materials, applications, and prospects. *Appl. Energ.* **236**, 489–513 (2019).
26. Raman, A. P. et al. Passive radiative cooling below ambient air temperature under direct sunlight. *Nature* **515**, 540–544 (2014).
27. Zhan, Z. B. et al. Enhancing thermoelectric output power via radiative cooling with nanoporous alumina. *Nano Energy* **65**, 104060 (2019).
28. Mu, E. Z. et al. A novel self-powering ultrathin TEG device based on micro/nano emitter for radiative cooling. *Nano Energy* **55**, 494–500 (2019).
29. Wang, T et al. A structural polymer for highly efficient all-day passive radiative cooling. *Nat. Commun.* **12**, 365 (2021).
30. Zhang, H. W. et al. Biologically inspired flexible photonic films for efficient passive radiative cooling. *Proc. Natl. Acad. Sci. U.S.A.* **117**, 14657–14666 (2020).
31. Ma, Q. L. et al. MOF-based hierarchical structures for solar-thermal clean water production. *Adv. Mater.* **31**, 1808249 (2019).
32. Kiani, F. et al. Ultra-broadband and omnidirectional perfect absorber based on copper nanowire/carbon nanotube hierarchical structure. *ACS Photonics* **7**, 366–374 (2020).
33. Li, D. et al. Scalable and hierarchically designed polymer film as a selective thermal emitter for high-performance all-day radiative cooling. *Nat. Nanotechnol.* **16**, 153–158 (2021).
34. Zhai, Y. et al. Scalable-manufactured randomized glass-polymer hybrid metamaterial for daytime radiative cooling. *Science* **355**, 1062–1066 (2017).
35. Y, Liu. et al. Ultrathin MEMS thermoelectric generator with Bi_2Te_3 /(Pt, Au) multilayers and Sb_2Te_3 legs. *Nano Convergence* **7**, 8(2020).

Figures

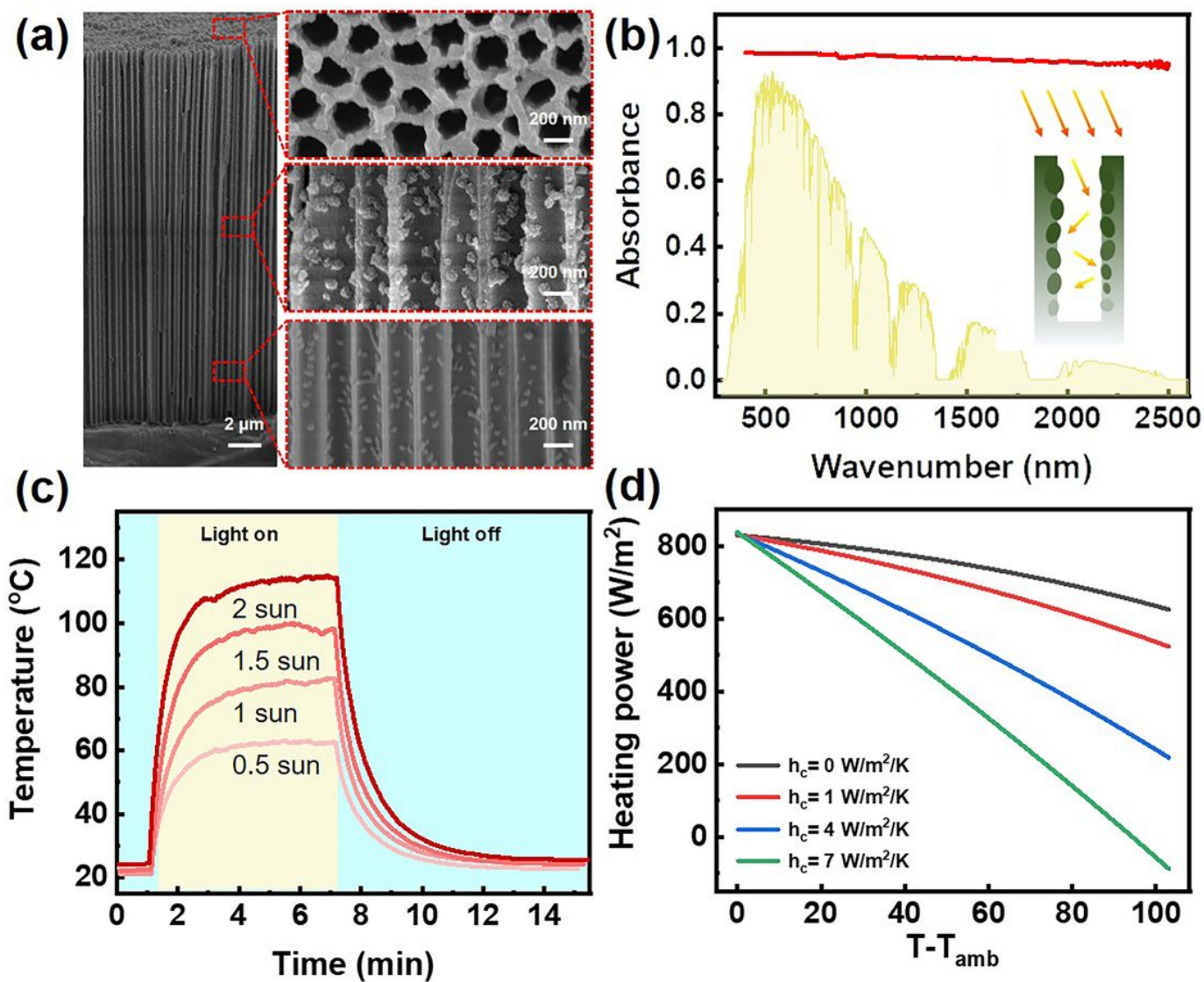


Figure 1

The microstructure and photothermal conversion performance of the solar absorber (PANI@AAO). (a) SEM images, (b) UV-vis-NIR absorption spectra and the schematic diagram of light-trapping effect, (c) surface temperature under different sun irradiation, (d) the calculated net heating power with different h_c (nonradiative heat coefficient) of the PANI@AAO.

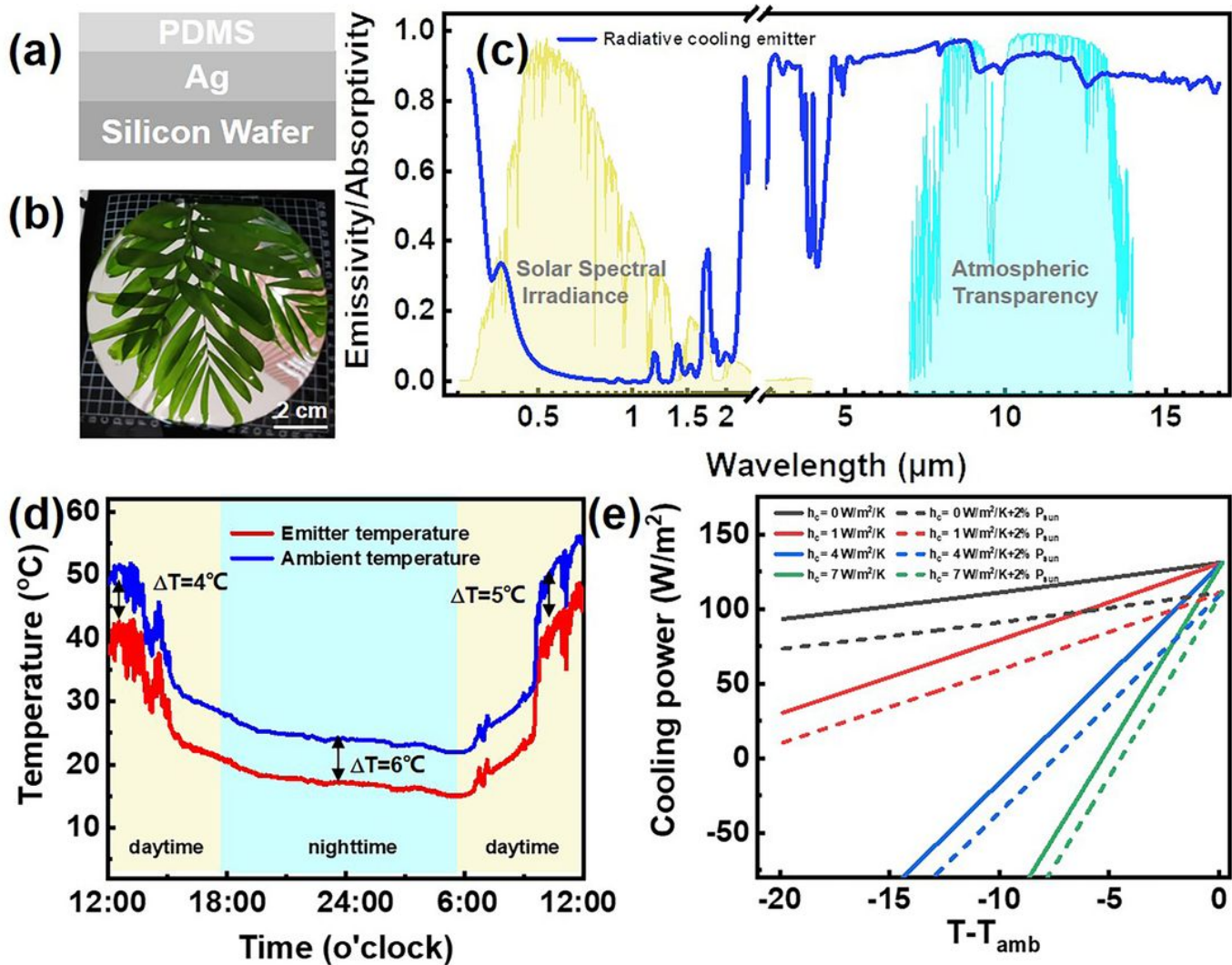


Figure 2

The structure and cooling performance of the radiative cooling emitter (PDMS-Ag). (a) The schematic diagram, (b) digital photo and (c) the measured emissivity/absorptivity spectra of the PDMS-Ag cooler. (d) Continuous measurement of the temperature tracking of the emitter and the ambient. (e) The calculated net cooling power during the nighttime (the solid line) and daytime (the dotted line).

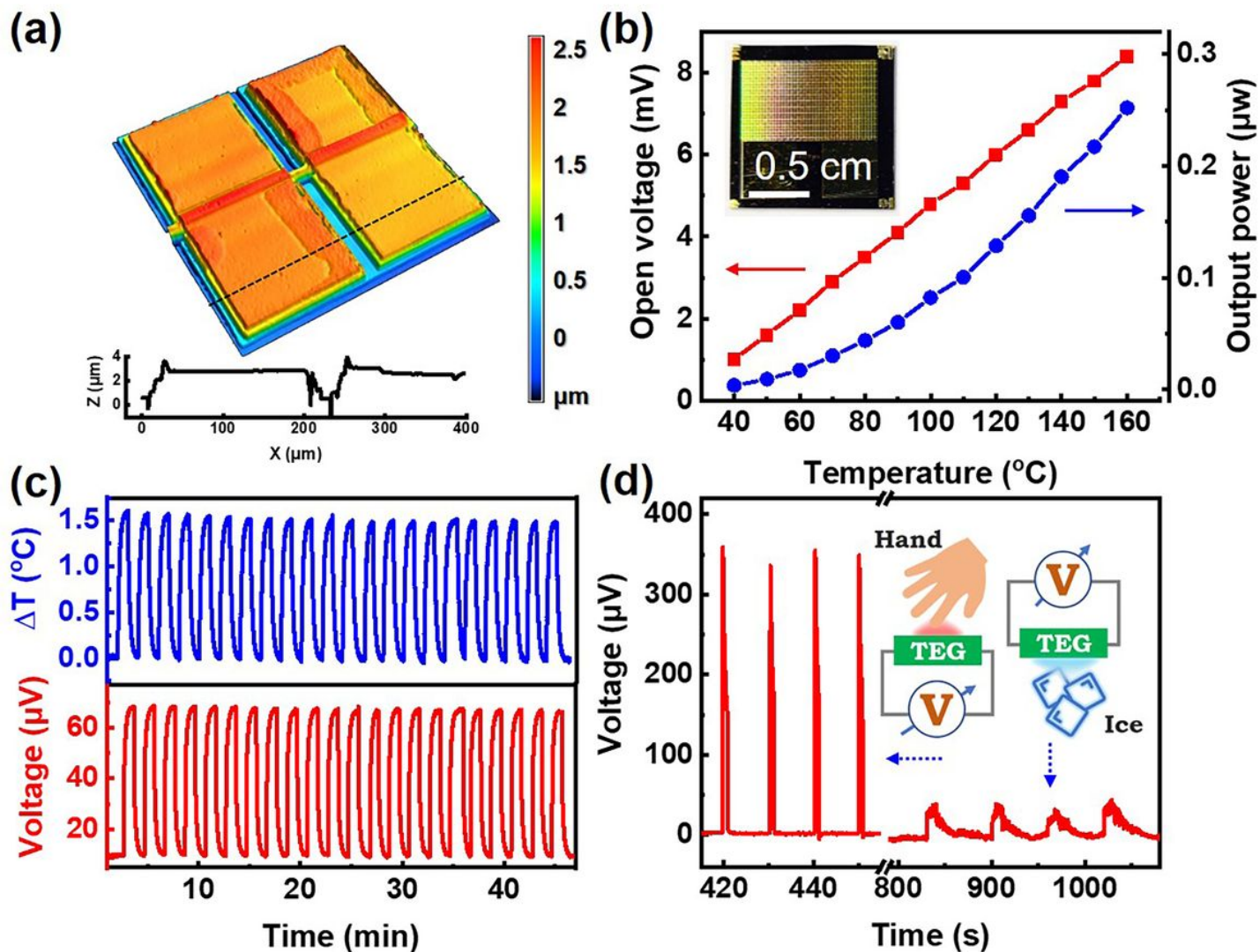


Figure 3

The structure and output performance of the ultrathin MEMS thermoelectric generator (TEG). (a) Surface profile of 2 P/N modules. (b) Open-circuit voltage and maximum output power, inset is the digital photo of TEG. (c) Reliability. (d) Sensitivity.

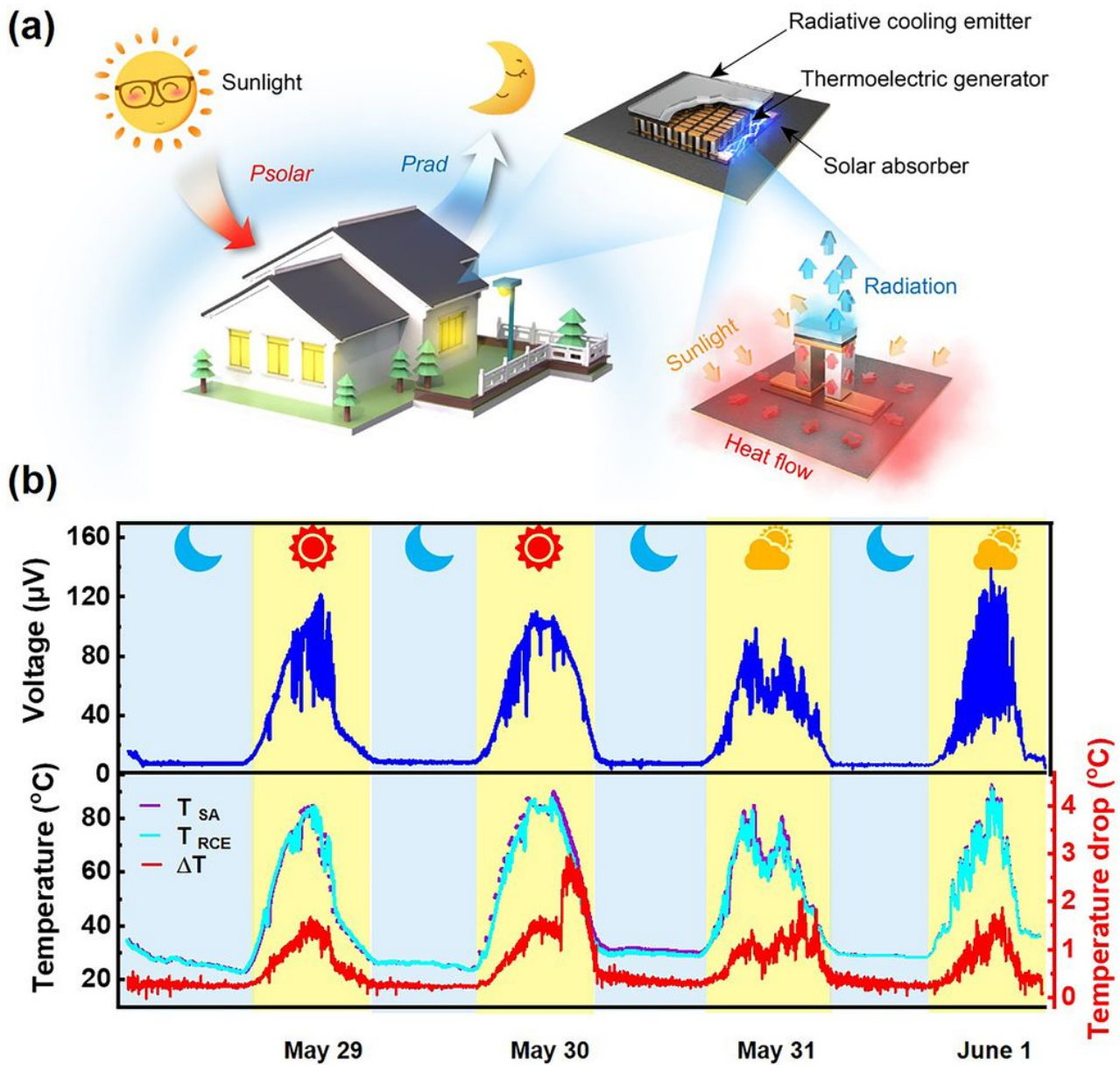


Figure 4

The concept and output performance of the all-day uninterrupted power generator. (a) Schematic of the self-generation power system in a building roof and the structure of the SA-RCE-TEG. (b) A 96-hour continuous measurement of the temperature of the SA and the RCE, and the output voltage of the SA-RCE-TEG in a real environment (from May 28 to June 1, 2021 in Shanghai).

Supplementary Files

This is a list of supplementary files associated with this preprint. Click to download.

- [20210813026supporting20210812.docx](#)

- [floatimage5.jpeg](#)